Polymer 50 (2009) 328–335

Contents lists available at ScienceDirect

Polymer

journal homepage: www.elsevier.com/locate/polymer

Off lattice Monte Carlo simulations of *AB* hybrid dendritic star copolymers

Leonidas N. Gergidis [a], Othonas Moultos [b], Costas Georgiadis [b], Marios Kosmas [b], Costas Vlahos [b,*]

[a] Department of Chemical Engineering, The Pennsylvania State University, University Park, PA 16802, USA
[b] Department of Chemistry, University of Ioannina, Ioannina 45110, Greece

ARTICLE INFO

Article history:
Received 22 September 2008
Received in revised form
25 October 2008
Accepted 27 October 2008
Available online 8 November 2008

Keywords:
Hybrid dendritic star copolymers
Monte Carlo simulations
Pivot algorithm

ABSTRACT

The conformational properties of Hybrid Dendritic Star copolymers (HDS) which combine the characteristics of dendrimers with those of flexible polymers are studied, for the first time, by means of Off Lattice Monte Carlo simulations. Using the efficient Pivot algorithm we calculate the asphericity and the acylindricity of the whole molecule for various solvent conditions and different characteristics of dendritic and star chains. Moreover, the effects of the number and the length of star branches on the conformation of the dendritic part are also studied. By considering the HDS copolymers as 'hairy spheres' we have calculated the star monomer distribution profiles. The shapes of the profiles are compared with previous Monte Carlo results.

1. Introduction

Dendrimers are highly branched macromolecules that are synthesized using a stepwise repetitive reaction sequence. This procedure leads to a very highly monodisperse polymer with a nearly perfect topology radiating from a central core and grown generation by generation [1]. The unique molecular structure of dendrimers with large number of terminal groups and well defined dimensions, surface and interior, offers potential applications in drug delivery systems, gene transfection, molecular containers, chemical catalysis, etc. [2,3]. In solutions, amphiphilic dendrimers designed with lyophobic interior and lyophilic exterior, have a size of a few nanometers and behave as unimolecular micelles [4]. The quest for larger self-assembled and self-organized systems to mimic nature's wisdom is an elusive and difficult objective in dendrimer chemistry and physics. Due to the progress in controlled polymer synthesis, new dendritic architectures incorporating linear polymer chains can be created [5–10]. These hybrid architectures combine the properties of dendrimers with those of flexible polymers. Hybrid copolymers are often designed to emulate macromolecular amphiphilies, with well-defined dendritic part that possesses hydrophobic or hydrophilic character and the linear chains possesses the opposite character. The addition of linear chains will drive the assembly behavior of these polymers in solution, in thin films and in the bulk resulting at first sight to many 'sophisticated' applications [11–13].

The conformational properties of hybrid star dendritic copolymers (Fig. 1) are also important. Depending on the dendrimer generation and the dendrimer branch length the linear chains can be found either in the interior or the exterior of the dendrimer radius of gyration. In the first case the shape of the hybrid molecule will be determined by the dendrimer characteristics. By increasing the linear chains length both parts the star and the dendrimer will influence the shape of the hybrid molecule. Further increase of the linear chain length will lead to a configuration similar to "hairy sphere" model [14] with the linear chains grafted in a dendrimer

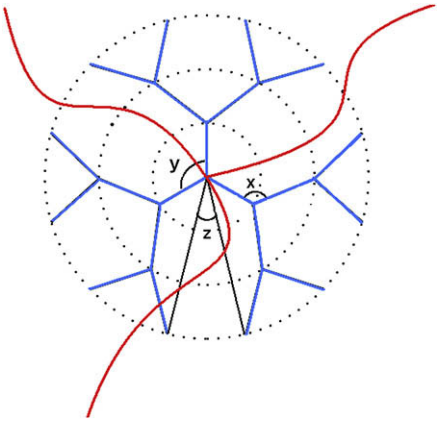

Fig. 1. Cartoon representation of the HDS copolymer containing trifunctional dendritic part of second generation and star part with 3 arms. The angles *X*, *Y* and *Z* are defined in the text (Section 3.2).

* Corresponding author. Tel.: +30 2651098430; fax: +30 2651098798.
E-mail address: cvlahos@cc.uoi.gr (C. Vlahos).

0032-3861/$ – see front matter © 2008 Elsevier Ltd. All rights reserved.
doi:10.1016/j.polymer.2008.10.055

spherical surface. Monte Carlo simulation results obtained with the cooperative motion algorithm [14] shows that the concentration profile of linear polymer units is sensitive both to the changes of interface radius and the surface coverage. For fixed chain length the monomer concentration profile changes from concave to convex as the radius of the sphere increases, and that the free chain ends are excluded from the neighborhood of the interface. The Monte Carlo simulations [14] lead to a simple model of the end-grafted chains. The first part of them tends to wrap around the sphere, the second gets coiled in the vicinity of the surface and the third forms the outer fraction of the elongated chains.

In previous studies [15,16], using Off Lattice Monte Carlo simulations we were able to simulate the conformational properties of dendrimers with polymeric length arms. The radii of gyration of different generations and of the whole dendrimer, the end-to-end square distances and various angles which describe the penetration of the end groups in the interior and the vacancies in the interior and exterior regions, were calculated using the efficient Pivot algorithm. Our results were in good agreement with respective analytical and experimental results [15]. In the current paper using the same algorithm we study the conformational properties of the hybrid *AB* star dendritic copolymers for various macroscopic states. The density profiles of the linear chain units, their end units, and the center of masses have been determined for different dendrimer generations and branch lengths. The asphericity and the acylindricity of both parts and of the whole molecule are also calculated. Finally, the influence of the number and the molecular weight of star branches on the conformational averages of dendritic part is studied.

2. Simulation model

We consider hybrid dendritic star copolymers containing a trifunctional dendritic part and *f*-functional star block (Fig. 1). Dendritic parts of different generations, *g*, equal to 1 and 2 with polymeric length branches are simulated, respectively. Each of the $3[2^{g+1}-1]$ dendritic branches contains N_D beads; the distance between neighboring beads is not constant but follows a Gaussian distribution with mean-root-square value *b* equal to the Kuhn length. For simplicity *b* is normalized to unity to facilitate future comparisons with analytic results. The central unit of the zeroth generation is the origin of coordinates and is assigned to be the unit $3[2^{g+1}-1]+1$. To this central unit *f* branches of the star part are attached. The star branch contains N_S beads where the bonds connecting neighboring beads also follow a Gaussian distribution with mean-root-square value *b*. The units of the dendrimer are assigned as *A-type* units and the respective units of the star chain as *B-type* units. Non-neighboring units interact through a 6–12 Lennard–Jones potential.

$$\frac{U(R_{ij})}{k_BT} = 4(\varepsilon_{kl}/k_BT)\left[\left(\frac{\sigma}{R_{ij}}\right)^{12}-\left(\frac{\sigma}{R_{ij}}\right)^{6}\right](k,l = A \text{ or } B), \quad (1)$$

where (ε_{kl}/k_BT) are the interaction energies between units of the same (*AA*, *BB*) or different homopolymers, R_{ij} is the separation distance between units *i* and *j*, and σ is a steric parameter (the diameter of the bead) considered the same for all units ($\sigma = 0.8$). Every set of values of interaction energies describes a different macroscopic state at which the hybrid *AB* dendritic star copolymer can exist. In previous studies of *AB* linear and miktoarm copolymers [17,18] we estimated the sets appropriate to reproduce the most important macroscopic states. We found that the macroscopic state of the selective solvent occurring frequently in real systems corresponds to a homopolymer part with *A–A* interactions under ideal Θ conditions, while *B–B* and *A–B* interactions are mainly repulsive. This state can be represented by the set $\varepsilon_{AA}/k_BT = 0, \varepsilon_{BB}/k_BT = 0.1, \varepsilon_{AB}/k_BT = 0.1$. The appropriate values describing the real pseudo-ideal theta of dendritic species or dendrimers are not known. For linear or star polymers these parameters are estimated from the exponent of the radius of gyration $\langle S^2\rangle \sim N^{2\nu}$ corresponding to the random walk value $\nu = 1/2$. In the case of the dendritic polymers the exponent of the radius of gyration even for the macroscopic state of good solvent is equal to 1/3 corresponding to bad solvent conditions of linear or star polymers. The reason why this is happening is that for dendritic molecules with molecular weights considered in the simulations the radius of gyration strongly depends on the number of dendritic arms (this is not the case of linear or star polymers). The omission of this term leads to unusual results for the exponent of the radius of gyration. Thus the value $\varepsilon_{ij}/k_BT = 0$, considered in the current work, leads to a safe description of theta solvent where no interactions between units are considered.

Another macroscopic state considered in this work is a common good solvent where all kinds of interactions are of the excluded volume type $\varepsilon_{kl}/k_BT = 0.1 (k,l = A \text{ or } B)$. Hybrid dendritic star copolymer chains containing dendrimers of first generation $g = 1$ and dendritic branch length equal to $N_D = 10$, 20, 30 and 40 units are simulated. The star chains contain up to 5 arms with lengths equal to $N_S = 10$, 20, 30, 50, 100 beads, respectively. For the second generation dendritic part $g = 2$ only the case with $N_D = 10$ is considered. The Monte Carlo algorithm initiates by building a hybrid dendritic star chain of moderate energy. The efficient Pivot algorithm [15–18] is used for the Monte Carlo sampling. Our previous study [15] of conformational properties of dendrimers based on the Bond fluctuation and the Pivot [24] algorithms shows that the latter is suitable for the study of dendritic polymers. Moreover the comparison with the free start-branched polymers and our available experimental results come to reinforce this conclusion. Other conformations are generated by randomly selecting either a dendritic or a star branch. A bond vector in the selected arm is chosen and its components are resampled from an appropriately chosen Gaussian distribution. The rest of the beads on the selected branch (and the units on the following arms if a dendritic arm is chosen) are rotated according to three randomly chosen Euler angles. The Metropolis energy criterion is used to test the acceptance or rejection of the new trial configuration. Ten independent runs are performed. Each run consists of between 1×10^7 and 5×10^7 Monte Carlo steps after appropriate thermalization. The properties of interest are initially averaged over all conformations in each run, and then the mean values and the standard deviations are determined based on the ten independent runs. The relative error of the calculated conformational properties varies between 0.9% and 7.8%, in general decreasing for higher values of the total molecular weight in general.

3. Results and discussion

3.1. Density profiles of star branches

The first property we computed was the monomer density profile $d_m(r)$ of the star chains for various macroscopic states as a function of the distance *r* from the central unit of the hybrid dendritic star (HDS) copolymer molecule. $d_m(r)$ is defined as [14]:

$$d_m(r) = \langle n_m\rangle(r)/n_{total}(r) \quad (2)$$

where $\langle n_m\rangle(r)$ denotes the average number of star chain beads as a function of the distance from the central unit between *r* and $r+dr$, n_{total} is the total number of beads with diameter σ which can be placed in this layer. The density profile of the free ends of star branches is defined similarly:

$$d_{fe}(r) = \langle n_{fe}\rangle(r)/n_{total}(r), \quad (3)$$

where $\langle n_{fe}\rangle(r)$ denotes their average number. The calculation of the density profiles is complemented by evaluating the distribution of star branches centers of mass related to volume $V(r)$

$$d_{cm}(r) = \langle n_{cm}\rangle(r)/V(r), \quad (4)$$

Fig. 2 presents the density profiles of the star units as a function of the distance from the HDS molecule central unit. The dendrimer is of first generation with arms containing $N_D = 10$ units. The HDS molecule is immersed in a selective solvent which is good for the dendrimer units and ideal theta for the star chain. The cross dendrimer-star interactions are considered to be repulsive. Fig. 2(a) refers to the monomer density profile $d_m(r)$ of star chains with functionality f varying from 1 to 5 and branch length $N_S = 20$. This length is equal to the dendrimer total arm length, starting from the central unit and terminating at the end unit of a first generation arm. It is observed that the monomer profile $d_m(r)$ is monotonically increasing function of the number of star arms f for fixed r, and monotonically decreases with r for fixed values of f. At a distance equal to the radius of gyration of the dendrimer $\langle S_D^2\rangle^{1/2}$, indicated by a vertical dashed line in the figure, the density has a significant value. We note that for shorter star arms equal to $N_S = 10$ (not presented in the figure) the majority of star units lies in the interior of the dendrimer radius and the density profile diminishes shortly after $r = \langle S_D^2\rangle^{1/2}$. For longer star arms ($N_S = 30$, 50 and 100) the monomer density, at distance $r = \langle S_D^2\rangle^{1/2}$, is increased. Eventually when $N_S = 100$ (Fig. 2(b)), $d_m(r)$ becomes three times higher from its respective value when $N_S = 20$, shown in Fig. 2(a).

The density profiles of star branches free ends, $d_{fe}(r)$, as a function of distance r from the central unit, are shown in Fig. 2(c) and (d), for $f \leq 5$ and $N_S = 20$ and 50, respectively. These density profiles are no longer monotonic functions of the distance r. The profiles increase from low values near the central unit up to a clear maximum at some r, and subsequently decrease to zero. The concentration of free ends at some distance r is strongly depended on the star branch length. For short branches the free ends concentrate at a distance between the central unit and the dendrimer radius of gyration. By increasing the branch length the distance where the concentration attains its maximum value, approaches the value of $\langle S_D^2\rangle^{1/2}$ and becomes equal for $N_S = 100$. Despite the fact that $d_{fe}(r)$ increases almost linearly as the number of star arms increases, the concentration distance is virtually independent of f.

In Fig. 3(a) and (b) we present the center of mass distributions, $d_{cm}(r)$, of the star chain branches. The profiles resemble those of the free ends of the previous section. With increasing r, $d_{cm}(r)$ raises up to a clear maximum and then goes down to zero. Both figures reveal a strong monotonic dependence of $d_{cm}(r)$ on the number of star branches. For shorter branches the maximum center of mass densities lie in a distance which is smaller than the dendrimer radius of gyration; in the case of $N_S = 100$ this maximum is located at the distance $\langle S_D^2\rangle^{1/2}$.

Fig. 4 depicts the density profiles of star branches for two different macroscopic states of selective solvent for the HDS copolymer. The first state, mentioned above, have star arms under ideal theta solvent while the dendrimer part is under good solvent conditions. The second macroscopic state is the reverse, with the dendrimer under ideal theta solvent and star branches under good solvent conditions. The interactions between dissimilar units are considered repulsive in both cases. Fig. 4(a) presents the monomer density profile $d_m(r)$ for a star chain with five branches, containing 50 beads each. The dendritic block is of first generation, having

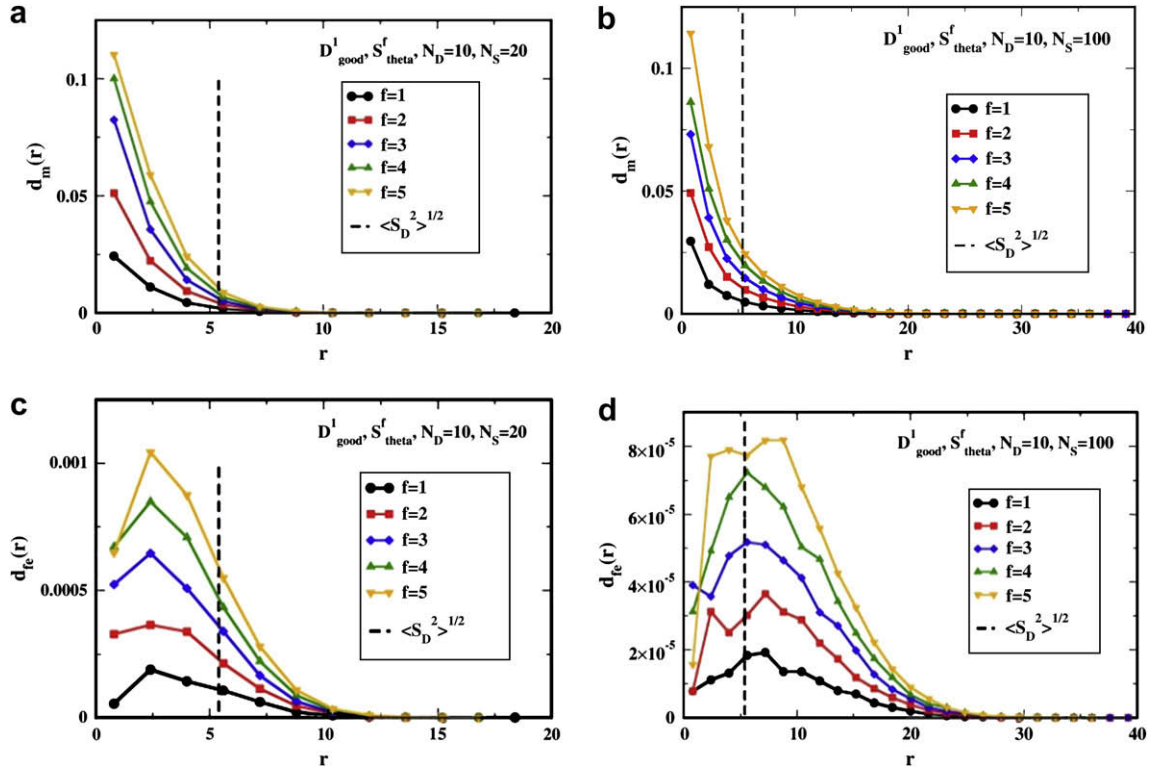

Fig. 2. (a) Star units density profiles $d_m(r)$ as a function of the distance r from the HDS molecule central unit for different number of star arms f. Symbols D^1_{good} and S^f_{theta} denote dendrimer of first generation under good solvent conditions and star with f branches under theta solvent, respectively. The dendritic and star arm lengths (N_D and N_S) are 10 and 20, respectively. $\langle S_D^2\rangle^{1/2}$ is the square root of the mean square radius of gyration of the dendritic part. (b) Same as in (a) except $N_S = 100$. (c) Density profiles of the free star branches ends $d_{fe}(r)$ vs. r. (d) Same as in (c) except $N_S = 100$.

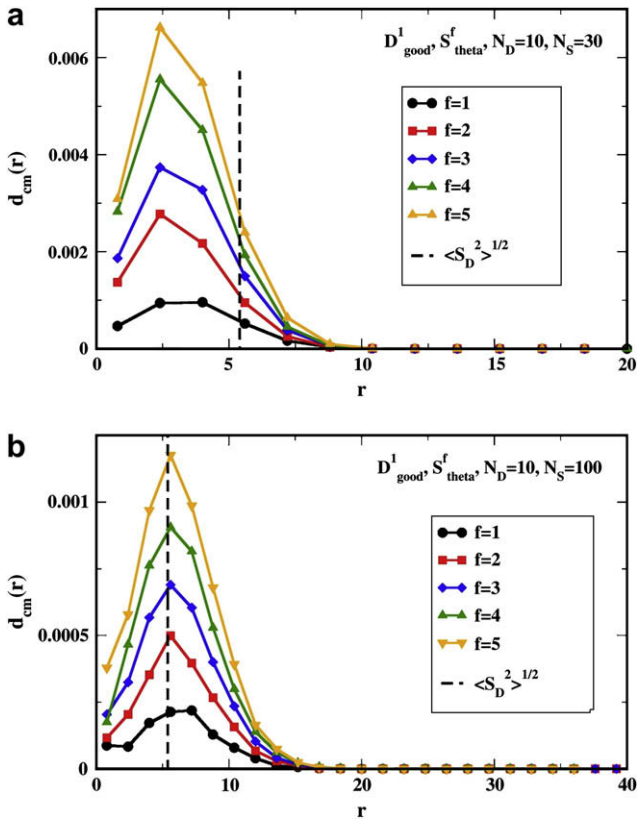

Fig. 3. (a) The star arms center of mass profiles as function or the distance r from the HDS molecule central unit. Notation is the same as Fig. 2(b) Same as in (a) except $N_S = 100$.

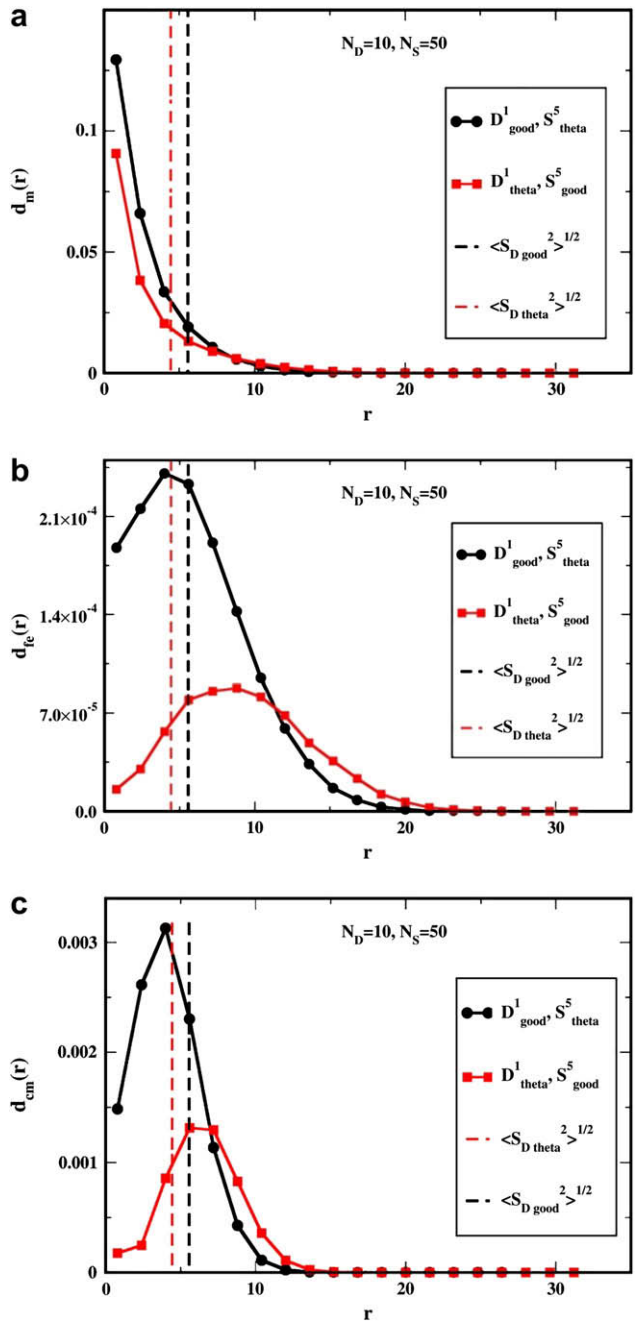

Fig. 4. (a) Star units' density profiles for two different selective solvents of the HDS copolymer as a function of distance r from the HDS central unit. (b) Density profiles of the free star branches ends vs. r for the two different selective solvents. (c) The star arms center of mass profiles as function or the distance r from the HDS molecule central unit. The notations are same as Fig. 2. In all cases the star part contains 5 arms.

arms of 10 beads. For a distance r exceeding both radii of gyration, $d_m(r)$ of the star chains under ideal theta conditions turns out to be larger than stars under good solvent condition. Then both distributions decay to zero, with that of ideal theta stars, in shorter distance r. The same trends are obtained irrespective of the number of star branches and their length. The concentration of star branches' free ends $d_{fe}(r)$ is illustrated in Fig. 4(b) for the same characteristics of the HDS molecule. Concentration of star branches' free ends, under ideal theta conditions, appears to be four times higher than this of branches in good solvent at distances around dendrimers radii of gyrations. Then both concentrations decay gradually and attain zero value when distance r is almost twice the $\langle S_D^2 \rangle^{1/2}$. For larger distances, $d_{fe}(r)$ of ideal branches approaches zero faster than $d_{fe}(r)$ of branches under good solvent conditions. $d_{cm}(r)$, distributions of branches under ideal theta and good solvent conditions are presented in Fig. 4(c). It can be observed that first one's profile takes higher values, than second's, for distances in the interior and neighborhood of dendrimers radii of gyration, due to the more coiled structure of ideal chains. For even greater distances the values of ideal branches $d_{cm}(r)$ become smaller than the respective of branches under good solvent conditions.

Subsequently the effects of heterointeractions were investigated, arising due to the differences of dendrimer size and dendrimer solvent conditions, on the monomer density of star chain. In Fig. 5(a) we present our results for HDS copolymers containing dendrimer of first generation with arm length $N_D = 10$, 20, 30 and 40 beads. The star chain has three branches, each one containing 100 beads. The solvent is ideal theta for the dendrimer and good for star chain. Interactions between dendrimer and star units are considered repulsive for all cases presented in Fig. 5. It can be seen that the differences among monomer density profiles are small and observable for distances smaller than the dendrimer radii of gyration and close to the HDS molecule central unit. At larger distances the profiles are virtually identical. This behavior leads to identical values for star block radii of gyration, confirmed also from separate calculations. This is due to the units lying in larger distances having a greater contribution to the radius of gyration tensor; thus any differences close to molecule's central unit are insignificant. Fig. 5(b) presents the distribution of star monomers for two different solvent conditions of the dendritic block. In the first case (common good solvent) all type of interactions considered repulsive. In the second case (selective solvent) no interactions are considered between the dendrimer units whereas B–B and A–B

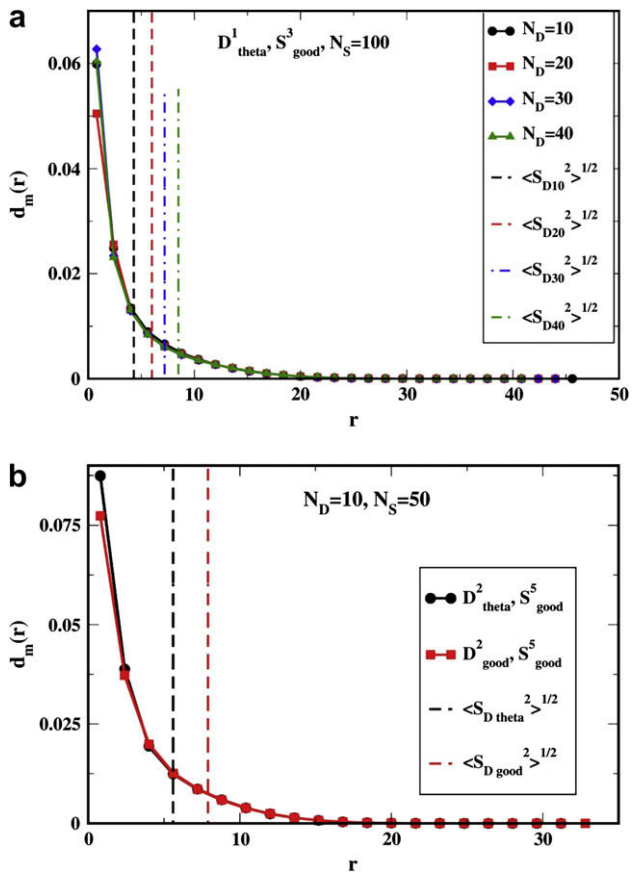

Fig. 5. (a) The star units' density profiles $d_m(r)$ as a function of distance r from the center of HDS molecule, for different dendritic arm lengths N_D. The star part contains 3 arms. (b) $d_m(r)$ vs. r for two different macroscopic states, the selective and common good solvents. The star part contains 5 arms while the dendritic part is of second generation.

interactions are of the excluded volume type. Both HDS molecules contain dendrimers of second generation with arm length $N_D = 10$ beads. The star chain contains five branches each one of which consists of $N_S = 50$ beads. Irrespective of dendrimer solvent conditions $d_m(r)$ the profiles are almost identical with only minor differences for distances smaller than dendrimers' radii of gyration. The current observations are in agreement with our previous results on linear or miktoarm star *AB* copolymers [17,18], where the radii of gyration of the two blocks are determined only from the type of intra-block interactions while the cross interactions have only marginal effect on the block size. If we consider the dendritic part as a sphere its radius R will be $(5/3)^{1/2}$ times greater than the root of the mean quadratic radius of gyration $\langle S_D^2 \rangle^{1/2}$. All monomer density profiles $d_m(r)$, studied in the present work, are concave functions of distance r. There is no monomer depletion observed near the dendrimer radius R (which is a convex function), contrary for the case of 'hairy spheres' with radius $R \geq 10$ polymer units [14]. The absence of monomer depletion can be explained by the following two reasons. All dendrimers radii of gyration studied regardless of generation and arm length have not exceeded the critical value of $(5/3)^{1/2}\langle S_D^2 \rangle^{1/2} = 10$. Additionally, dendrimers of small generation are not exactly hard spheres, permitting easily the back-folding of star beads.

3.2. Dendrimer conformation

The purpose of the present section is to describe and analyze dendrimer conformation of the HDS copolymer based on the three different angles *X*, *Y*, *Z*, shown in Fig. 1. For an in-depth study and discussion on the angles the interested reader can refer to [15,16,19]. Moreover the dendrimer radius of gyration, mean asphericity A_{sph} and acylindricity A_{cyl} are calculated with the aim to study the effect of the star branches on the size and shape of the dendritic block. The aforementioned angles can be used in order to specify (to a first approximation), the relative positions of the ends of dendrimer arms, the available space in the interior of the dendritic polymer and its capability to carry guest molecules.

When the angle *X* is large the end beads are mainly located at the outside region of the dendrimer and they are very active; for small values of *X* they turn inside the dendrimer matrix and their activity is hindered. The angle *Y*, between the position vectors of the two ends of the arms of the zeroth generation, indicates the free spaces that the interior region can have. For larger angles *Y*, larger available space in the interior of the dendritic part is expected. Hence, the capability to carry guest molecules is higher. Angle *Z*, formed by the vectors connecting the central unit with the end bead of different dendrons can provide information about the entry of cargo to the interior of the dendritic molecule.

In Fig. 6 we present results for HDS copolymers containing dendrimer of first generation with arm length $N_D = 10$ and star chains, with varying branch number, containing $N_S = 100$ beads each. HDS copolymer is studied for two different selective and a common good solvents, with all heterointeractions considered to be repulsive. For an ideal dendrimer all angles are equal to $\pi/2$. In Fig. 6(a) we observe that the presence of an interacting star with one branch under good solvent conditions is not affecting angle *Y*. The increase of *f*, however, leads to a significant decrease of *Y*. The reason is that the increase of the number of star units, with repulsive heterointeractions, reduces the available space of the dendrimer units of the zeroth generation leading to smaller *Y* angles.

For the macroscopic state of common good solvent, the increase of the number of star branches has marginal effect on the angle *Y*. The reason is in the common origin of the zeroth generation arms, which forces them to be spatially close. Because of the proximity of the arms, repulsions between the monomeric beads, force these specific arms to extend outwards. This extension permits the ends of these arms to approach, increasing the *Y* angle, compared to the previous macroscopic state. The placement of the star arms, which are also much stretched with the majority of their units placed out of the radius of gyration of the interior generation, has no significant effect on the angle *Y*.

In the second case of selective solvent, dendrimer under good solvent conditions and ideal star branches, the increase of their number leads to a decrease of *Y*. This is due to the fact that the star chain is not stretched; thus many star units are placed close to the interior dendrimer arms decreasing their available space.

Angle *X*, between mean end-to-end square distances of the two successive generations, attains higher values with the increase of the number of star arms *f*. This observation is indicative of the stretching of the pairs of successive arms due to the increase of repulsions between the star and dendritic units (Fig. 6(b)). The stretching is more intense when dendrimer is under good solvent conditions and star branches under ideal theta solvent conditions, less intense for HDS under common good solvent and weaker for the reverse selective solvent with ideal theta dendrimer and star branches in good solvent.

The effects of the number of star arms on the angle *Z* are illustrated in Fig. 6(c). Angle *Z* increases as *f* increases for all macroscopic states studied. The repulsive heterointeractions make the exterior arms more extended thus the ends of the outer arms approach with increasing angle *Z*. Angle *Z* is wider in the case of ideal dendrimer since the outer arms and their ends can be closer. In common good solvent, this angle becomes smaller due to the repulsive interactions between monomeric units.

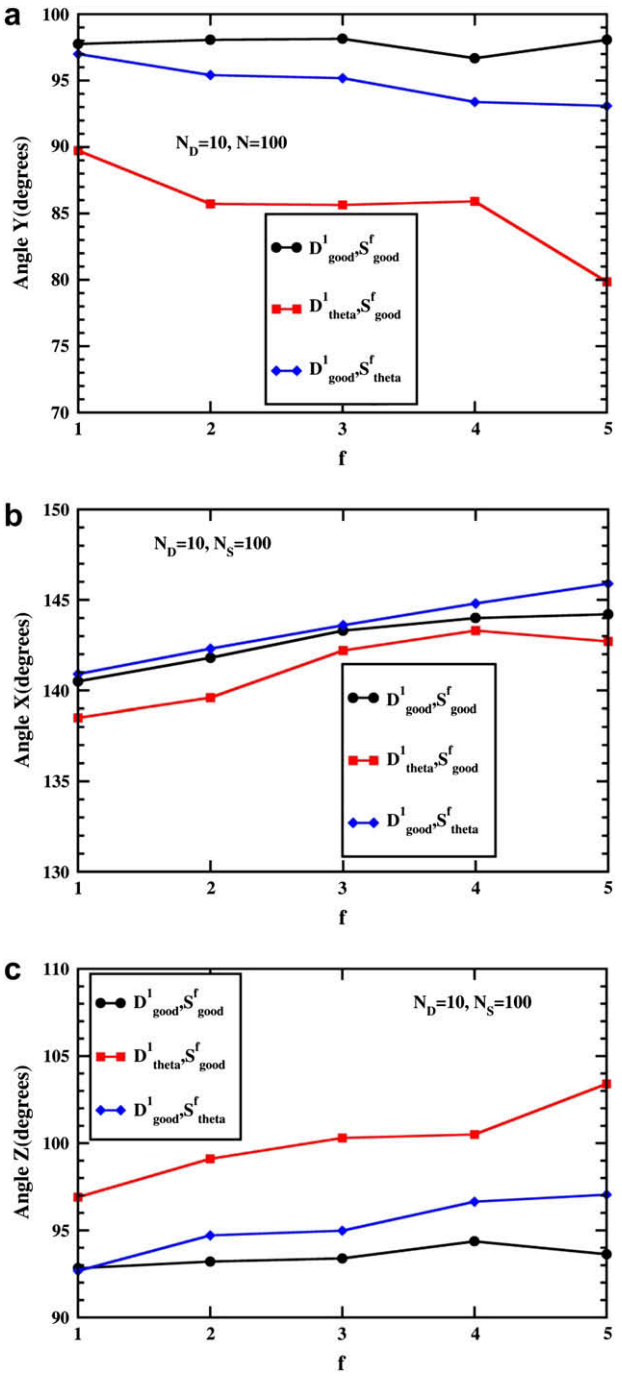

Fig. 6. The dependence of the dendrimer angles *X*, *Y* and *Z* on the functionality *f* of star chains for different solvent conditions. The notation is same as above.

In the case of an HDS copolymer with ideal star branches the values of *Z* angle are higher than the respective values for the macroscopic state of common good solvent. The available volume of the outer generation is higher since the ideal star branches are permitted to overlap. The same trends for the angles *X*, *Y* and *Z* obtained for HDS copolymers containing dendrimers of second generation.

Other properties that were also studied include the radius of gyration, the asphericity and the acylindricity of the whole dendrimer chain. Based on references [20,21], the asphericity *Asph* and acylindricity *Acyl* are computed using the principal components of the mean square radius of gyration tensor S_x^2, S_y^2 and S_z^2, where $S_x^2 > S_y^2 > S_z^2$.

$$A_{\mathrm{sph}} = \left[< S_x^2 > -\frac{1}{2}\left(< S_y^2 > + < S_z^2 > \right) \right] / < S^2 > , \quad (5)$$

$$A_{\mathrm{cyl}} = \left(< S_y^2 > - < S_z^2 > \right) / < S^2 > , \quad (6)$$

For a rigid rod, acylindricity is zero and asphericity is near one. For spheres, both acylindricity and asphericity are near zero.

In Fig. 7(a) we present results for the dendrimer mean radius of gyration. HDS copolymers contain star block with up to five branches, with lengths varying from 10 to 100 units. The dendrimer is of the first generation with arm length equal to 10 units. The

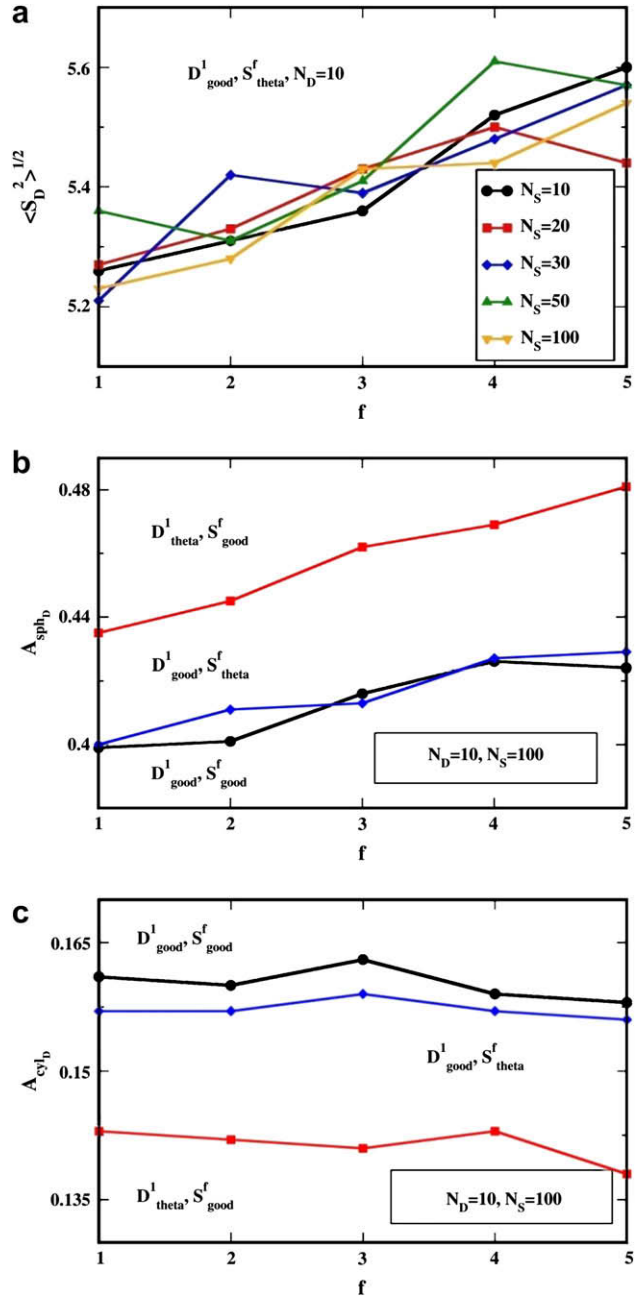

Fig. 7. (a) The dependence of the square root of the mean square radius of gyration of the dendritic part on the functionality *f* of star block for different star arm lengths. (b) The asphericity of the dendritic block as a function of *f*, for three different macroscopic states. (c) The acylindricity of the dendritic block as a function of *f*, for three different macroscopic states.

solvent is good for dendrimer and ideal theta for the star chain. It can be seen that the increase of f leads to a small increase of the radius of gyration around 8%. This increase is almost independent of the star branch length, since for long star branches ($N_S = 50, 100$) the majority of units are far apart of the dendritic ones, reducing the number of heterointeractions.

The asphericity of the dendritic part of second generation with $N_D = 10$ is presented in Fig. 7(b) only for long star branches ($N_S = 100$) for all solvent conditions. In all cases the asphericity is increasing almost linearly with the increase of star arms. The increase is greater for ideal dendrimer and smaller for the HDS under common good solvent. The dendrimer then becomes less spherical since the radial density distribution profiles of star and dendritic units are different. Thus increasing the star units, the space available for dendritic units is less spherically symmetric resulting to the increase of dendrimer asphericity. The acylindricity values show virtually no change when the number of star branches increases (Fig. 7(c)).

3.3. The shape of HDS copolymer

The shape of the whole HDS copolymer molecule depends on dendrimer characteristics, the number and the length of star branches and the solvent conditions. In Fig. 8(a) and (b) we present our results for asphericities and acylindricities the of HDS copolymers containing dendrimer of first generation with arm length $N_D = 10$ units. The solvent is good for the dendrimer and theta for the star arms while the interactions between dissimilar units are considered repulsive. In the case of one long star branch ($N_S = 100$) the value of the asphericity of HDS molecule is about 0.6 which is higher than the respective value of linear chain under theta conditions (0.526) [22,23]. Also the acylindricity equal to 0.137 indicating a "tadpole like" shape. For $f = 2$ the HDS asphericity becomes equal to the one of linear chains. Further increase of f leads to decreased values of A_{sph} and in the case of $f = 3$ becomes equal to the respective value of the dendrimer block. For $f = 5$ the HDS asphericity is 0.37, while the A_{sph} of ideal star chains is 0.22 [22,23]. For shorter star arms ($N_S = 50$), the HDS asphericity in all cases is smaller than the dendrimer asphericity and also smaller than a chain with $N_S = 100$. The lowest value of asphericity is obtained for star branch length $N_S = 30$ which is 30% higher than the dendrimer total arm length. Asphericity of star branches with $N_S = 20$, which is equal to total dendrimer arm length, takes values close to $N_S = 30$. The shortest star branches ($N_S = 10$), which lie in the interior of the dendrimer, have weaker influence on the HDS shape when the number of star branches increases.

Similar trends are obtained for HDS copolymers containing dendrimer of second generation. In Fig. 8(c) we present results for the same macroscopic state of selective solvent. In all cases asphericity takes lower values compared to the respective asphericities of HDS, containing first generation dendrimer, due to the more spherical dendritic part. The most spherical conformation is obtained for HDS copolymers with $N_S = 50$, length which exceed the total dendrimer arm ($N_D = 30$). Short star branches containing 10 units have very small influence on the HDS shape. The case of HDS copolymer with $N_S = 100$ is of some importance. Its asphericity for $f = 5$ is smaller or equal to the asphericities of copolymers with shorter arms (up to $N_S = 30$). This peculiar behavior not observed to the respective HDS copolymer containing dendrimer of first generation may be explained as follows: The long arms have

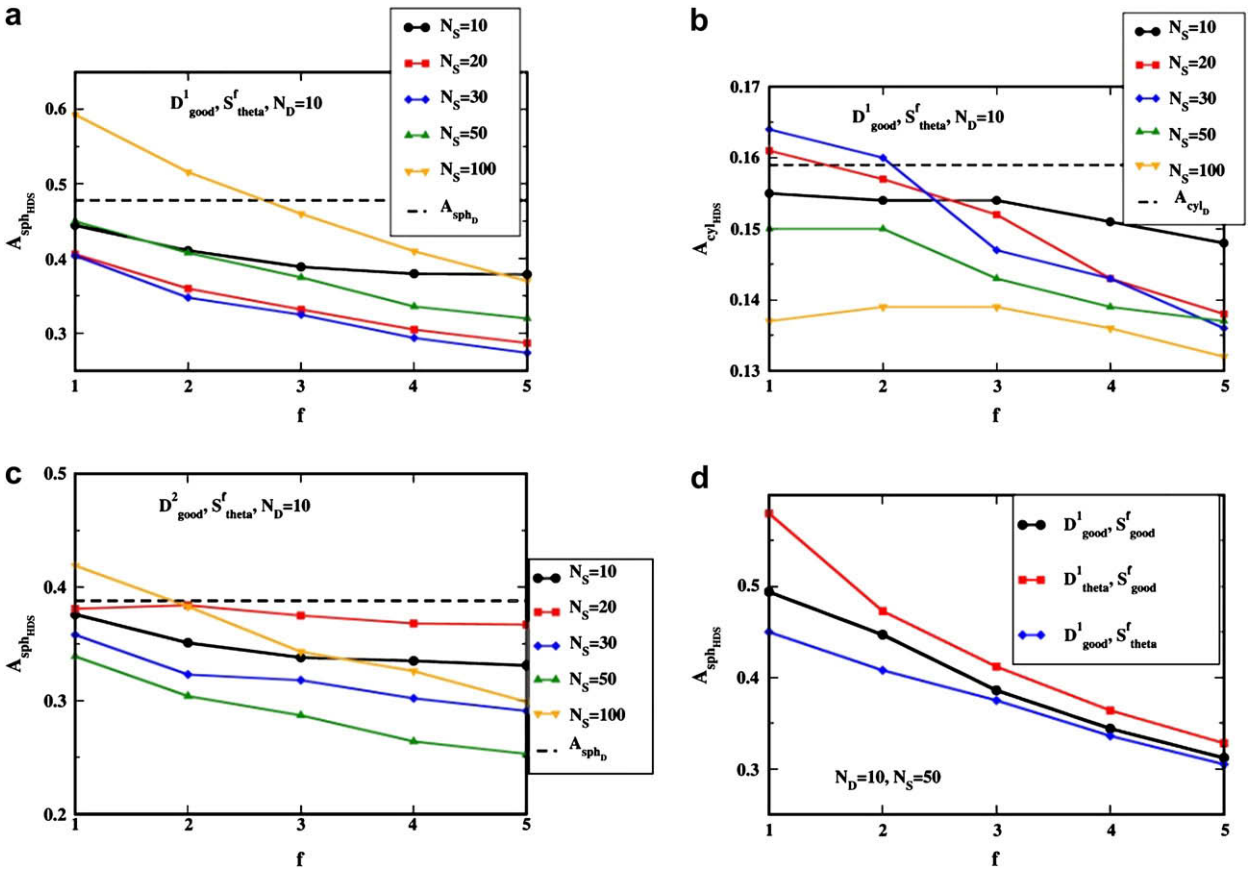

Fig. 8. (a) The dependence of the asphericity of the dendritic part on the functionality f of star block for different star arm lengths. (b) The dependence of the acylindricity of the dendritic part on the functionality f of star block for different star arm lengths. (c) The same as (a) but for second generation dendritic block. (d) The dependence of the asphericity of the dendritic part on the functionality f for three different macroscopic states.

a greater ability to wrap around the dendrimer compared to the shorter ones. The dendrimer of second generation appears to be more spherical in comparison with the respective of first generation, thus the star branches wrapped around a more spherical object may lead to smaller asphericity of the HDS copolymer.

The effects of the solvent on the HDS asphericity are presented in Fig. 8(d) for various macroscopic states. The dendritic part is of first generation while the star chain branches contain $N_S = 50$ units. The highest values of asphericity are obtained for HDS copolymers with the dendritic part under ideal theta conditions. The lowest values are obtained for copolymers with dendrimers under good solvent with ideal star branches. This is due to the fact that dendrimers under good solvent are more spherical compared to the ones under ideal theta conditions whereas the ideal star branches are easily wrapped around of the dendritic part leading to more spherical shape. The asphericity of HDS under common good solvent conditions lies between the values of the two different selective solvents. However for HDS molecules containing star chains with many branches, the differences in the asphericity become very small and the effects of the solvent conditions become negligible.

4. Conclusions

The conformational properties of HDS copolymers, which combine the characteristics of dendrimers with those of flexible star polymers, were studied with Off Lattice Monte Carlo simulations. We found that the star units' density profile is a concave function with respect to the distance r from the HDS central unit. Star monomer depletion near the dendrimer surface is not observed, as in the case of "hairy spheres", due to the small number of generations of our dendritic blocks.

The conditions under which the star branches' free ends concentrate at distance smaller, equal to or higher than the square root of the mean square radius of gyration of the dendritic part, are defined for different macroscopic states. We also found that the number and length of the star branches has a small effect on the conformation of the dendrimer block.

The shape of the HDS copolymer changes from "tadpole-like" to almost spherical when the number of star arms increases. HDS shape is more spherical in comparison with the dendritic block's shape, for star arm lengths exceeding 30% of the total dendritic arm length.

Acknowledgment

We would like to thank Professors A. Charalambopoulos and A. Armaou for helpful discussions. The Research Center for Scientific Simulations (RCSS) of the University of Ioannina is gratefully acknowledged for providing the computer resources used in this work.

References

[1] Tomalia DA, Naylor AM, Goddard WA. Angw Chem Int Ed Engl 1990; 29:138–75.
[2] Frechet JMJ, Tomalia DA. Dendrimers and other dendritic polymers. New York: Wiley; 2001.
[3] Patri AK, Majoros IJ, Baker JR. Curr Opin Chem Biol 2002;6:466–71.
[4] Frechet JMJ, Hawker CJ, Wooley KL. J Macromol Sci Pure Appl Chem 1994;A31:1627–45.
[5] Frauenrath H. Prog Polym Sci 2005;30:325–84.
[6] Andreopoulou AK, Carbonnier B, Kallitsis JK, Pakula T. Macromolecules 2004;37:3576–87.
[7] Gao Y, Xiwen Z, Miao Y, Xinjun Z, Wei W. Macromolecules 2007;40:2606–12.
[8] Osano K, Turner R. J Polym Sci Part A Polym Chem 2008;46:958–69.
[9] Yu D, Vladimirov N, Frechet JMJ. Macromolecules 1999;32:5186–92.
[10] Ge Z, Luo S, Liu S. J Polym Sci Part A Polym Chem 2006;44:1357–71.
[11] Namazi H, Adeli M, Zarnegar Z, Jafari S, Dadkhah A, Shukla A. Colloid Polym Sci 2007;285:1527–33.
[12] Adeli M, Zarnegar Z, Dadkhah A, Hossieni R, Salimi F, Kanani A. J Appl Polym Sci 2007;104:267–72.
[13] Suek NW, Lamm MH. Langmuir 2008;24:3030–6.
[14] Klos J, Pakula T. J Chem Phys 2003;118:7682–9.
[15] Rangou S, Theodorakis PE, Gergidis LN, Avgeropoulos A, Efthymiopoulos P, Smyrnaios D, et al. Polymer 2007;48:652–63.
[16] Efthymiopoulos P, Vlahos C, Kosmas M, Gergidis LN. Macromolecules 2007;40:9164–73.
[17] Vlahos C, Horta A, Molina L, Freire J. Macromolecules 1994;27:2726–31.
[18] Vlahos C, Tselikas Y, Hadjichristidis N, Roovers J, Rey A, Freire J. Macromolecules 1996;29:5599–604.
[19] Kosmas M, Vlahos C, Avgeropoulos A. J Chem Phys 2006;125:094908.
[20] Tanaka G, Mattice WL. Macromol Theory Simul 1996;5:499–523.
[21] Theodorou DN, Suter UW. Macromolecules 1984;18:1206–14.
[22] Bishop M, Clarke J, Rey A, Freire J. J Chem Phys 1991;94:4009–11.
[23] Jagodzinski O. J Phys A Math Gen 1994;27:1471–94.
[24] Freire JJ, Pla J, Rey A, Prats R. Macromolecules 1986;19:452–7.